Pergamon

Bioorganic & Medicinal Chemistry 9 (2001) 647–651

BIOORGANIC & MEDICINAL CHEMISTRY

The Crystal Structure of the Complex of Non-peptidic Inhibitor of Human Neutrophil Elastase ONO-6818 and Porcine Pancreatic Elastase

Y. Odagaki,[a,*] K. Ohmoto,[a] S. Matsuoka,[b] N. Hamanaka,[a] H. Nakai,[a] M. Toda[a] and Y. Katsuya[c]

[a]*Minase Research Institute, Ono Pharmaceutical Co., Ltd. 3-1-1 Sakurai, Shimamoto-Cho, Mishima-Gun, Osaka 618–8585, Japan*
[b]*Development Headquarters, Ono Pharmaceutical Co., Ltd. 2-1-5 Doshou-machi, Chuo-Ku, Osaka-City, Osaka 541–8526, Japan*
[c]*Hyogo Prefectural Institute of Industrial Research, 3-1-12 Ikuhira-Cho, Suma-ku, Kobe-City, Hyogo 654–0037, Japan*

Received 13 September 2000; accepted 14 October 2000

Abstract—The crystal structure of a new inhibitor of human neutrophil elastase (HNE), N-[2-[5-(*tert*-butyl)-1,3,4-oxadiazol-2-yl]-(1*RS*)-1-(methylethyl)-2-oxoethyl]-2-(5-amino-6-oxo-2-phenyl-6*H*-pyrimidin-1-ly)acetamide (ONO-6818, **1**) complexed to porcine pancreatic elastase (PPE) has been determined at 1.86 Å resolution. Analytical results provided evidence of a 1:1 complex in which the electrophilic ketone of **1** covalently bound to Oγ of Ser195 at the active site of PPE. The role of the unique electron-withdrawing ketone of **1** has been elucidated.

Introduction

Human neutrophil elastase (HNE, EC.3.4.21.37) is a serine protease produced by neutrophils in response to inflammatory stimuli.[1] Excessive production of elastase has been implicated in the etiology of various diseases such as emphysema,[2] adult respiratory distress syndrome (ARDS),[3] cystic fibrosis[4] and rheumatoid arthritis.[5] A low molecular weight inhibitor of elastase would prove therapeutically useful against such pathologies.[6,7] In 1996, we reported an intravenously active HNE inhibitor **4** (ONO-5046, Fig. 1) which exhibited clinical efficacy in the treatment of acute lung injury caused by systemic inflammatory response syndrome (SIRS), idiopathic pulmonary fibrosis (IPF) and chronic airway infection.[8] The development of an orally active inhibitor of HNE has long been a challenge for medicinal chemists all over the world. A large number of synthetic inhibitors of elastase have been reported.[9] However, orally active inhibitors with clinical potential are very rare. The only successful example was peptidyl trifluoromethyl ketone (TFMK) **2a** (Fig. 1), reported by ZENECA.[10]

Recently, we reported the design and synthesis of a new non-peptidic, orally active inhibitor of HNE.[11] Among several compounds tested, N-[2-[5-(*tert*-butyl)-1,3,4-oxadiazol-2-yl]-(1*RS*)-1-(methylethyl)-2-oxoethyl]-2-(5-amino-6-oxo-2-phenyl-6*H*-pyrimidin-1-ly)acetamide **1** (ONO-6818, Fig. 1) provided the most attractive oral profile. For example, it was orally active at a dose of 1.4 mg/kg (ED_{50}) in an acute hemorrhagic assay. Compound **1**, α-keto-5-*tert*-butyl-1,3,4-oxadiazole, has a structurally unique heterocyclic electron-withdrawing moiety compared to TFMK. An analysis of X-ray crystal structure of the newly discovered inhibitor complexed to porcine pancreatic elastase (PPE, EC.3.4.21.36) is of particular significance to elucidate its mechanism of inhibition at the molecular level. Compound **1** has structural novelty, potent inhibitory activity ($K_i = 12.2$ nM),[11] and more than 100-fold the selectivity for HNE of other human proteases such as pancreatic elastase, proteinase 3, trypsin, metalloelastase, Cathepsin G, plasmin, thrombin and collagenase. We report herein a crystallographic study of the orally active non-peptidic inhibitor of HNE **1** complexed to PPE.

Results and Discussion

As shown in Figure 2, substrate-based electrophilic ketone inhibitors of HNE[8] consist of three portions: P3–P2, P1(Val) and an electron-withdrawing moiety such as trifluoromethyl[10,12,13,17] or oxadiazole.[14–16] Sometimes an

*Corresponding author. Tel.: +81-75-961-1151; fax: +81-75-962-9314; e-mail: odagaki@ono.co.jp

0968-0896/01/$ - see front matter
PII: S0968-0896(00)00277-7

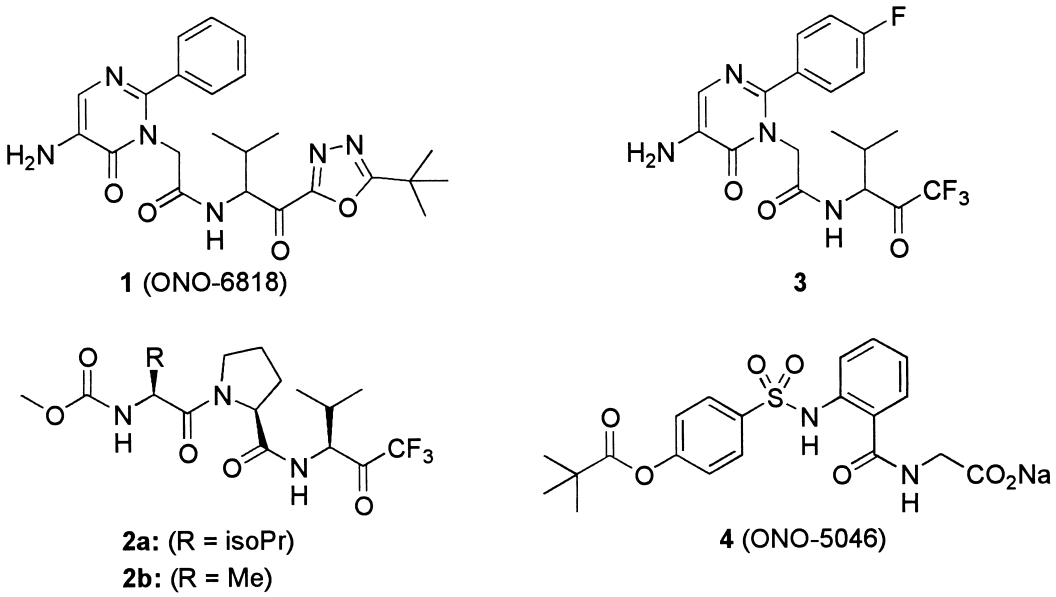

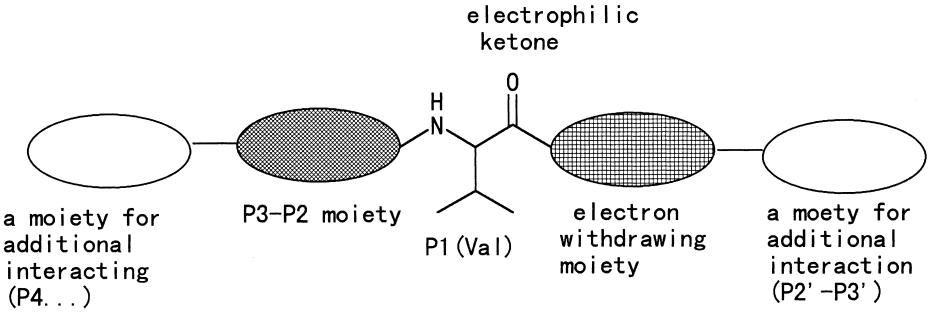

Figure 2. A schematic diagram of substrate-based electrophilic ketone

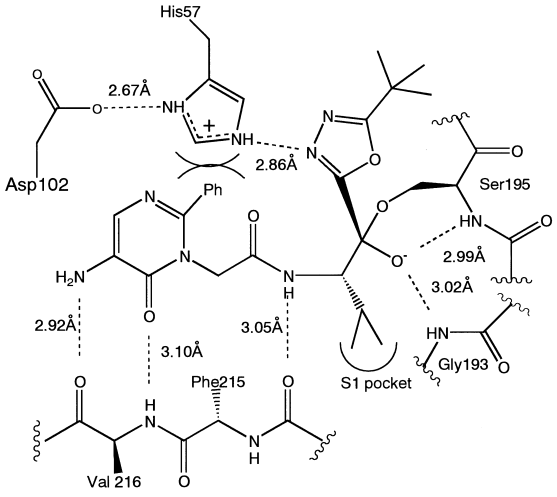

Figure 3. (a) A schematic diagram of the binding interactions found in the crystal structure of **1**/PPE complex. The dashed lines represent the hydrogen bonds. The side chain of P1(Val) was inserted into the S1 pocket of PPE. The π–π and/or van der Waals interaction was also observed between the imidazole ring on His57 and the phenyl ring of **1**.

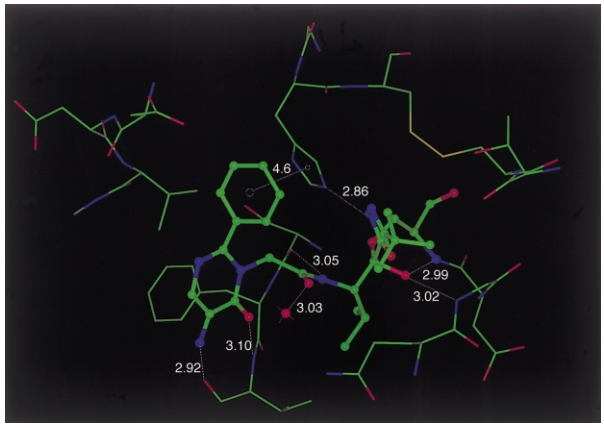

Figure 3. (b) The relationship between positon-2 phenyl ring of the pyrimidinone of **1** and imidazole ring of His57.

additional moiety (P2′–P3′) is beneficial for further optimization of the inhibitory activity and/or physical properties of the inhibitors as illustrated by the *tert*-butyl group of **1**. Peptidic inhibitors have a Val-Pro (**2a**[17]) or Ala-Pro (**2b**[18]) residue at P3-P2 and two reciprocal hydrogen bonds were observed between P3(Ala/Val) of the inhibitor and Val216 of PPE.[14,17] The P3–P2 portion could be replaced by the heterocylic ring moiety without loss of the β-strand conformation. The 5-amino-2-phenylpyrimidin-6-one moiety of the TFMK inhibitor **3**[19] reported by ZENECA scientists was is representative of the replacements.[12,13,19–21]

The hydrogen bond network of **1** complexed to PPE is demonstrated in Figure 3a and 3b. The phenyl ring at position-2 of the pyrimidinone is beneficial to the interaction with HNE (Fig. 3b). While the side chain methylene of the Pro at position P2 of the peptidic inhibitor (**2a**[17] and **2b**[18]) is exposed to solvent region, π-π interaction and/or van der Waals' interaction between the phenyl ring of **1** and the imidazole ring of His57 of PPE was observed in **1** complexed to PPE (Fig. 3b). The distance between the centers of the two rings was 4.6 Å, while the distance between the two atoms of each ring located in the closest position was 3.7 Å. The inter-plane angle was 45°. These interactions were beneficial for the stabilization of the complex consisting of **1** and PPE. The temperature factor of the phenyl ring atoms was reasonably low (around 20 $Å^2$ for each atom). The carbonyl oxygen of the Gly moiety of **1** did not interact with PPE, while it formed a hydrogen bond with a water molecule.

The electron density map of the isopropyl group of P1(Val) of **1** was unambiguous and easily assigned (Fig. 4a). While we used the racemic compound for crystallization, only the *S*-isomer of **1** was observed at the active site of PPE. An excess molar amount of **1** was used for co-crystallization, and the electron density of the *R*-isomer of **1** was not found even at the surface of PPE. The chiral center of P1(Val) could be easily epimerized at room temperature.[11]

A covalent bond was formed between the hydroxyl group of Ser195 of PPE and the P1(Val) ketone carbonyl of **1** (Fig. 4). The carbonyl carbon atom of P1 of **1** was found to be SP.[3] The hemiketal oxyanion of the tetrahedral intermediate was located at the oxyanion hole of PPE.[14,16,20] Hydrogen bonds were observed between the hemiketal oxyanion of **1** and two amide protons of Ser195 and Gly193. The distance between the hemiketal oxyanion of **1** and the amide proton of Ser195 and of Gly 197 was 2.99 and 3.02 Å, respectively.

The newly discovered inhibitor **1** contains α-keto-1,3,4-oxadiazole as a unique electron-withdrawing moiety. Replacement of the TFMK moiety of **3** with 5-*tert*-butyl-1,3,4-oxadiazole provided **1** with nearly 10 times more activity in vitro than **3**.[11] The oxadiazole ring seems to contribute not only to the electrophilicity of the ketone moiety but also to the stabilization of the

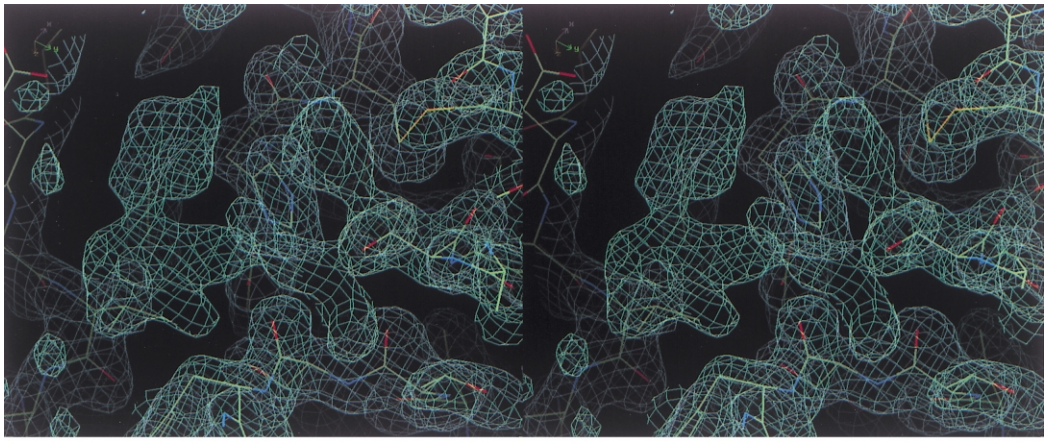

(a)

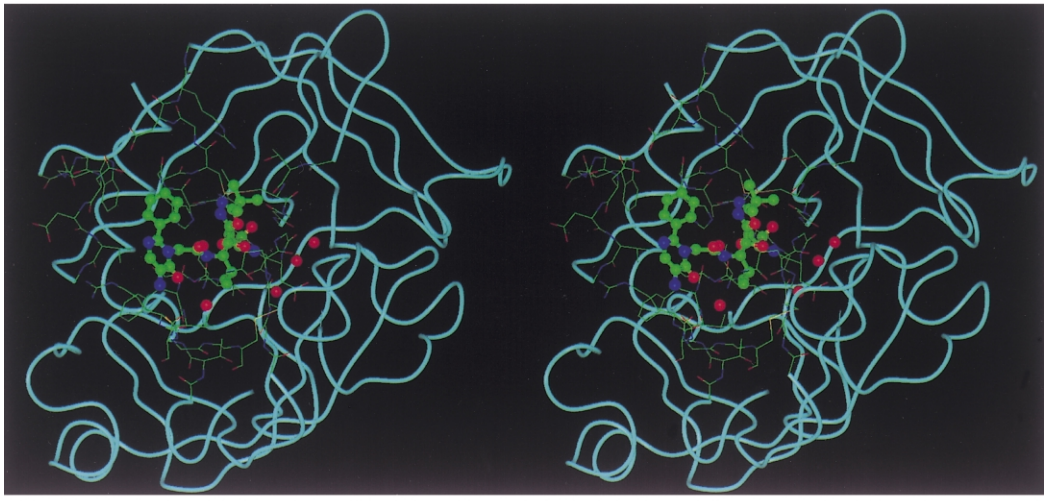

(b)

Figure 4. (a) The omit-refine map of the active site region of **1**/PPE complex; (b) the stereo drawing of the active site region of **1**/PPE complex. **1** is shown with the ball and stick model, and active site residue of PPE is shown with the wire model.

intermediate by forming a hydrogen bond (Fig. 3a and b). The active site of PPE consists of the suitable coordination of the catalytic triad residues, His57, Asp102 and Ser195.[9] The configuration of catalytic triad residues could overlap among the substrate-based electrophilic ketone inhibitor and apo PPE. The hydrogen bond distance between position-3 of the oxadiazole ring of **1** and Nε2 of the imidazole ring of His57 was 2.86 Å. The distance between Oγ of Ser195 and Nε2 of His57 of the **1**/PPE complex was 3.27 Å and it is slightly longer than that of apo PPE. On the other hand, the distance between Nδ1 of His57 and Oδ1 of Asp102 was 2.67 Å in the **1**/PPE complex structure. The distance is almost same as that of apo PPE structure.

According to the mechanism of hydrolysis, both nitrogen atoms of the imidazole ring of His57 are considered to undergo proton abstraction from the hydroxyl group of Ser195 when the tetrahedral intermediate forms. After the proton of Nε2 of His57 moves back to the Oγ of Ser195, the inhibitor is released from the active site of the enzyme. The basicity of the nitrogen atom of the oxadiazole ring is considered to prevent the proton from migration by hydrogen bonding. As a result, the tetrahedral intermediate is thought to be stabilized.

The tertiary butyl group was exposed to solvent region. No specific interaction with PPE was observed. However, the structure–activity relationship suggested the importance of this part.[11] This group may have a role in positioning the oxadiazole ring by steric hindrance effect.

The crystal structure of 1

The crystal structure of **1** was determined (Fig. 5). All the torsion angles of **1** were similar to those of **1** complexed to PPE except for the torsion angle of the Cα–Cβ bond of P1(Val) (Fig. 6). The SP^2 carbonyl carbon atom of P1(Val) was converted to SP^3 to form a covalent bond to the Oγ oxygen of Ser195. The crystal structure of **1** showed a folded shape enabling the phenyl ring of P2–P3 and the oxadiazole ring to interact. The Val side chain of **1** protruded from the folded molecule. The folded shape was speculated to be retained also in aqueous phase. As shown in the crystal structure of **1** complexed to PPE (Fig. 1), the distance between the position-2 carbon atom of the 2-phenyl ring on the pyrimidinone ring and the position-3 nitrogen atom of the oxadiazole ring was 3.72 Å. The distance between the position-3 carbon atom of the phenyl ring and position-4 nitrogen atom of the oxadiazole ring of the free form of **1** was 3.57 Å. The inter-plane angle of these two rings was 58.8°. These values seem to be appropriate for the two aromatic rings to interact. This folded molecular shape may force the Val side chain (P1Val) to obtain access to the S1 pocket of PPE/HNE. As such, **1** may be expected to inhibit the enzyme relatively with faster binding manner compared to TFMK inhibitor **3**.

Further refinement will be considered based on these results, and reported in due course.

Experimental

PPE was purchased from Roche Diagnostics and used for crystallization without further purification. Synthesis of **1** will be reported elsewhere.[11] Compound **1** was synthesized as a racemic form because of its easily enolizable structure. To a solution of lyophilized PPE (10 mg) in a 10 mM sodium acetate buffer (pH 5.0), a 10-fold molar excess of **1** in acetonitrile was added. Crystals were grown using the hanging drop vapor diffusion method with an aqueous solution of sodium sulfate solution (10 g/100 mL w/v) as precipitant. Crystals were directly mounted from the drop in thin walled glass capillaries. X-ray diffraction data from a single crystal were collected at room temperature with an *R*-axis IV imaging plate area detector using Ni-Filtered Cu K_α radiation (an Rigaku RU200 X-ray generator operating at 40 kV and 100 mA). The raw data were processed and merged using the Rigaku-processing program. The final *R*-merge value was 5.5%. The data were 98.8% complete to 1.86 Å; the final shell data from 1.92 to 1.86 Å, were 96.0% complete. The total number of reflections collected was 19,460 (Table 1).

Refinement

Refinements were carried out using program X-PLOR.[22] The program QUANTA/X-ray[22] was used for electron density fitting and drawing pictures. The

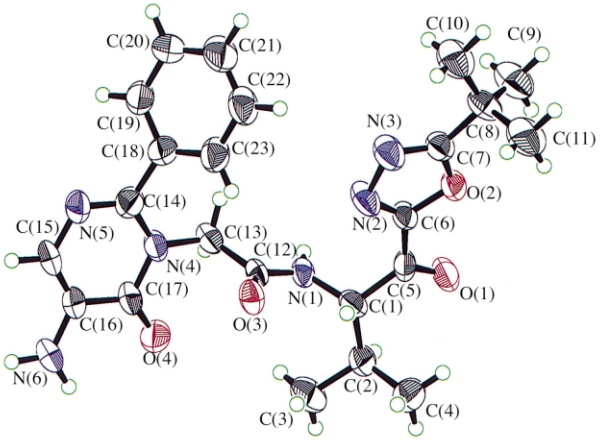

Figure 5. The ORTEP drawing of **1** with thermal ellipsoids at 50% probabilities.

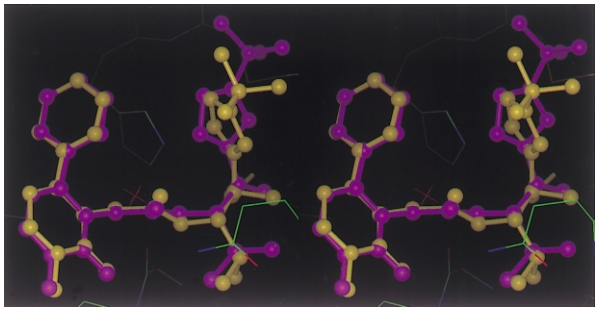

Figure 6. The superimposed models of **1** (purple)/PPE complex and **1** (yellow).

Table 1. The crystallographic data of **1**/PPE complex and **1**

X-ray data		**1**/PPE	**1**
Space group		Orthorombic $P2_12_12_1$	Monoclinic $P2_1/a$
Cell dimension	*a*	51.037(3) Å	9.687(5) Å
	b	58.500(3) Å	12.210 (4) Å
	c	75.6427(2) Å	19.320 (3) Å
	β		95.47(2)°
No. of mol/asymm unit		1	1
Resolution/$2\theta_{max}$		1.86 Å	130.1°
R-merge		5.5%	
Completeness		98.8%	
No. of reflections[a]		19460	3832
Rcryst		19.9%	7.0%
Free*R*/w*R*		23.8%	5.8%
RMSD[b]	Bond length	0.005 Å	
	Angle	1.33°	
Average B (main chain)		21.6 (for 961 atoms)	
Factor (Å^2) (side chain)		25.0 (for 861 atoms)	
	(Inhibitor **1**)	21.9 (for 33 atoms)	
	(Water)	25.1 (for 64 atoms)	

[a]Number of collected reflections.
[b]Deviations from ideal values.

program Insight II[22] was also used for drawing pictures. The crystallographic parameter was listed (Table 1). The isomorphous native PPE coordinates were initially taken as the starting set for calculating structure factors, *Fc*s. After several cycles, a difference Fourier map was calculated. The electron density at the active site clearly indicated that a complex formed. Also, the continuous density from Oγ of Ser195 indicated covalent binding of **1** to Oγ of Ser195.

The X-PLOR parameters for the inhibitor were estimated from the crystal structure of **1** and the parameters reported by Edwards et al.[14] Compound **1** was modeled to fit electron density in the active site. The modeled inhibitor was included in further cycles of refinement; an initial temperature factor of 20 Å^2 was assigned to all non-hydrogen atoms of the inhibitor. Only the water molecules presenting at a contour level of 3σ on the $|Fo|-|Fc|$ map were retained. Several cycles of positional and temperature factor refinement were calculated. The final *R* factor and free *R*-factor were 0.198 and 0.238, respectively. The final refinement statistics are also given in Table 1. The omit-refine map of the active site region of **1** bound to PPE is in Figure 4a.

X-ray crystallography of 1

Pale yellow single crystals were obtained from an *N*,*N*-Dimethylformamide solution of **1**. Diffraction data were collected using a Rigaku AFC5R 4-circle diffractometer with an RU-200 X-ray generator. An empirical absorption correction was applied. The data were also corrected for Lorentz and polarization effect. The program package teXsan[23] was used for analysis and drawing figures. The positions of non-H atoms were easily determined by the program SHELXS86,[24] and the positions of the H atoms were deduced from coordinates of the non-H atoms and confirmed by Fourier synthesis. The non-H atoms were refined with anisotropic temperature parameters. H atoms were included for structure factor calculations but not refined.

References

1. Travis, J.; Dubin, A.; Potempa, J.; Watorek, W.; Kurdowska, A. *Ann. N. Y. Acad. Sci.* **1991**, *624*, 81.
2. Janoff, A. *Am. Rev. Repir. Dis.* **1985**, *132*, 417.
3. Merritt, T. A.; Cochrane, C. G.; Holcomb, K.; Bohl, B.; Hallman, M.; Strayer, D.; Edwards, D.; Gluck, L. *J. Clin. Invest.* **1983**, *72*, 656.
4. Jackson, A. H.; Hill, S. L.; Afford, S. C.; Stockley, R. A. *J. Respir. Dis.* **1984**, *65*, 114.
5. Ekerot, L.; Ohlsson, K. *Adv. Exp. Med. Biol.* **1984**, *167*, 335.
6. Edwards, P. D.; Bernstein, P. R. *Med. Res. Rev.* **1994**, *14*, 127.
7. Bernstein, P. R.; Edwards, P. D.; Williams, J. C. *Progr. Med. Chem.* **1994**, *31*, 59.
8. Sakuma, T.; Takahashi, K.; Ohya, N.; Usuda, K.; Handa, M.; Abe, T. *Eur. J. Pharmacol.* **1998**, *353*, 273.
9. For a comprehensive review of synthetic HNE inhibitors, see: (a) Metz, W. A.; Peet, N. P. *Exp. Opin. Ther. Patents* **1999**, *9*, 851. and the references cited therein. (b) Skiles, J. W.; Jeng, A. Y. *Exp. Opin. Ther. Patents* **1999**, *9*, 869 and the references cited therein.
10. Edwards, P. D.; Andisik, D. W.; Bryant, C. A.; Ewing, B.; Gomes, B.; Lewis, J. J.; Rakiewicz, D.; Steelman, G.; Strimpler, A.; Trainor, D. A.; Tuthill, P. A.; Mauger, R. C.; Veale, C. A.; Wildonger, R. A.; Williams, J. C.; Wolanin, D. J.; Zottola, M. *J. Med. Chem.* **1997**, *40*, 1876.
11. Ohmoto, K.; Yamamoto, T.; Horiuchi, T.; Imanishi, H.; Odagaki, Y.; Kawabata, K.; Sekioka, T.; Hirota, Y.; Matsuoka, S.; Nakai, H.; Toda, M. *J. Med. Chem.*, in press.
12. Bernstein, P. R.; Gomes, B. C.; Kosmider, B. J.; Vacek, E. P.; Williams, J. C. *J. Med. Chem.* **1995**, *38*, 212.
13. Edwards, P. D.; Andisik, D. W.; Strimpler, A. M.; Gomes, B.; Tuthill, P. A. *J. Med. Chem.* **1996**, *39*, 1112.
14. Edwards, P. D.; Meyer, E. F. Jr.; Vijayalakshmi, J.; Tuthill, P. A.; Andisik, D. A.; Gomes, B.; Strimpler, A. *J. Am. Chem. Soc.* **1992**, *114*, 1854.
15. Edwards, P. D.; Wolanin, D. J.; Andisik, D. W.; Davis, M. W. *J. Med. Chem.* **1995**, *38*, 76.
16. Edwards, P. D.; Zottola, M. A.; Davis, M.; Williams, J.; Tuthill, P. A. *J. Med. Chem.* **1995**, *38*, 3972.
17. Cregge, R. J.; Durham, S. L.; Farr, R. A.; Gallion, S. L.; Hare, C. M.; Hoffman, R. V.; Janusz, M. J.; Kim, H.-O.; Koehl, J. R.; Mehdi, S.; Metz, W. A.; Peet, N. P.; Pelton, J. T.; Schreuder, H. A.; Sunder, S.; Tardif, C. *J. Med. Chem.* **1998**, *41*, 2461.
18. Takahashi, L. H.; Radhakrishnan, R.; Rosenfield, R. E., Jr.; Meyer, E. F. Jr.; Trainor, D. A.; Stein, M. *J. Mol. Biol.* **1988**, *201*, 423.
19. Brown, F. J.; Andisik, D. W.; Bernstein, P. R.; Bryant, C. B.; Ceccarelli, C.; Damewood, J. R. Jr.; Edwards, P. D.; Earley, R. A.; Feeney, S.; Green, R. C.; Gomes, B.; Kosmider, B. J.; Krell, R. D.; Shaw, A.; Steelman, G. B.; Thomas, R. M.; Vacek, E. P.; Veale, C. A.; Tuthill, P. A.; Warner, P.; Williams, J. C.; Wolanin, D. J.; Woolson, S. A. *J. Med. Chem.* **1994**, *37*, 1259.
20. Bernstein, P. R.; Andisik, D.; Bradley, P. K.; Bryant, C. B.; Ceccarelli, C.; Damewood, J. R. Jr.; Earley, R.; Edwards, P. D.; Feeney, S.; Gomes, B. C.; Kosmider, B. J.; Steelman, G. B.; Thomas, R. M.; Vacek, E. P.; Veale, C. A.; Williams, J. C.; Wolanin, D. J.; Woolson, S. A. *J. Med. Chem.* **1994**, *37*, 3313.
21. Veale, C. A.; Bernstein, P. R.; Bryant, C.; Ceccarelli, C.; Damewood, J. R. Jr.; Earley, R.; Feeney, S. W.; Gomes, B.; Kosmider, B. J.; Steelman, G. B.; Thomas, R. M.; Vacek, E. P.; Williams, J. C.; Wolanin, D. J.; Woolson, S. *J. Med. Chem.* **1995**, *38*, 98.
22. Molecular Simulations Inc.: San Diego, CA.
23. Molecular Structure Corporation.: The Woodlands: TX.
24. Sheldrick, G. M. In *Crystallographic Computing 3*; Sheldrick, G. M., Kruger, C., Goddard, R., Eds.; Oxford University Press: 1985, pp. 175–189.